

PROGRESS IN THE PREDICTION OF UNSTEADY HEAT TRANSFER  
ON TURBINES BLADES

T. Cebeci  
California State University  
Long Beach, California

R.J. Simoneau  
NASA Lewis Research Center  
Cleveland, Ohio

and

A. Krainer and M.F. Platzer  
Naval Postgraduate School  
Monterey, California

This presentation describes the progress toward developing a general method for predicting unsteady heat transfer on turbine blades subject to blade-passing frequencies and Reynolds numbers relevant to SSME, such as illustrated in figure 1. The method employs an inviscid/viscous interactive procedure (fig. 2) which has been tested extensively for steady subsonic and transonic external airfoil problems. One such example is shown in figure 3. The agreement with experimental data and with Navier-Stokes calculations yields confidence in the method. The present work extends the technique to account for wake generated unsteadiness. The flow reversals around the stagnation point caused by the nonuniform onset velocity are accounted for by using the Characteristic Box scheme developed by Cebeci and Stewartson. The coupling between the inviscid and viscous methods is achieved by using a special procedure, which, with a novel inverse finite-difference boundary-layer method, allows the calculations to be performed for a wide range of flow conditions, including separation.

Preliminary results are presented for the stagnation region of turbine blades for both laminar and turbulent flows. A laminar model problem corresponding to a flow on a circular cylinder which experiences the periodic passing of wakes from turbine blades is presented to demonstrate the ability of the method to calculate flow reversals around the stagnation region. Calculations cover a Strouhal number range of 0.1 to 0.2 and a leading-edge Reynolds number range of  $2 \times 10^4$  to  $4 \times 10^5$ .

#### BASIC EQUATIONS

The basic equations are presented in figure 4. As an essential preliminary to more extensive calculations involving complete blades, we consider here the development of an unsteady boundary-layer method for calculating the flow properties near the stagnation region of a blade where the movement of the stagnation point with space and time poses problems. We assume that the external velocity distribution is represented in dimensionless form by a function

(eq. (1)) which allows the variation of the stagnation point and the free-stream velocity.

For a two-dimensional, incompressible time-dependent laminar flow, the boundary-layer equations and their boundary conditions are well known, and for conditions with no mass transfer and specified wall temperature they can be written in the form shown in equations (2) to (6).

The calculation of upstream boundary conditions in the  $(t,y)$  plane at some  $x = x_0$  when the conditions at a previous time line are known can introduce different problems. To illustrate these difficulties for the case of a moving stagnation point, let us consider equation (1). Since  $u_0 = 0$  at the stagnation point by definition, its location based on the external streamlines is given by  $\xi_s = B(\tau)$ .

Figure 5 shows the variation of the stagnation point with time according to the equation with  $B(\tau) = 1 + c \sin \omega\tau$ ,  $c = 1$ ,  $\omega = \pi/4$ . We see that the stagnation point  $\xi_s$  is at 2 when  $\tau = -2$  and at 0 when  $\tau = 6$ , etc. If  $\xi_s$  were fixed, we could assume that  $u = 0$  at  $\xi_s = -1$  for all time and for all  $y$ , but this is not the case.

It is more convenient and useful to express equations (2) to (5) in a form more suitable for computation. To achieve this, we introduce the dimensionless variables  $\tau$ ,  $\xi$ ,  $\eta$ ,  $w$ ,  $m$ , and  $G$  together with a dimensionless stream function  $f(\xi, \eta, \tau)$  and, with  $\theta = \partial f / \partial \xi$ , write equations (2) to (5) as shown in equations (7) to (9). We use the Characteristic Box method to avoid the numerical problems associated with flow reversals in the stagnation region and to generate the initial conditions on the next time "line." This scheme requires that equations (7) and (8) are expressed in terms of new coordinates. For this purpose, we note the definition of local streamlines and let  $d\tau = d\xi/f'$ . If the distance in this direction is designated by  $s$  and the angle that it makes with the  $\tau$ -axis by  $\beta$ , then the transformed momentum and energy equations (7) and (8) and their boundary conditions can be written as shown in equations (10) to (13).

## MODEL PROBLEM

To illustrate the method we introduce a model problem, which corresponds to a flow on a circular cylinder of diameter  $D$ , which experiences the periodic passing of the wakes from the turbine blades (see fig. 6). For a time period  $t_g$  the cylinder is subjected to a freestream velocity  $U_\infty$  and for  $t_w$  it is immersed in a superimposed moving wake which has a motion component  $u_b$ . The cycle repeats itself with a so-called blade passing frequency  $F[\equiv 1/(t_g + t_w)]$  and is related to the Strouhal number  $St$  by  $FD/U_\infty$ . We assume that the stagnation region of the cylinder is subjected to a velocity which varies in space and time according to equation (1). (The variables are listed in fig. 6.)

Calculations are made for two values of Strouhal number taken equal to 0.1 and 0.2 with the dimensionless minimum wake velocity  $u_m = 1/3$  in both cases. The computed values of wall heat flux  $G'(0)$  show that they are not influenced by the changes in the freestream velocity and are virtually constant for the range of  $\xi$  and  $\tau$  values considered with  $G'(0) \sim 0.50$  for  $St = 0.1$  and  $G'(0) \sim 0.51$  for  $St = 0.2$ .

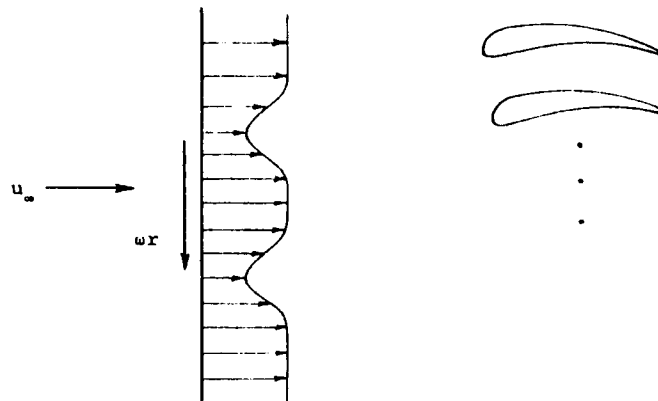
As shown in figure 7, the computed values of wall shear  $f''(0)$  for  $St = 0.1$  are significantly influenced by the changes in the freestream velocity which causes flow reversals in the velocity profiles around the stagnation point based on the vanishing of the external velocity. The movement of the stagnation point and the resulting flow reversals increase with time and with space. For example, the calculations for steady state have the stagnation point at  $\xi = 0$ , and, as expected, there is no flow reversal in either side of the stagnation point. At  $\tau = 0.05$ , the stagnation point moves to  $\xi = 0.15$  but the flow reversals in the velocity profiles continue up to and including  $\xi = 0.85$  as can be seen from the results shown in figure 8.

### CONCLUDING REMARKS

The computed results show that the numerical procedure is able to obtain solutions for a range of blade-passing frequencies of practical relevance. The movement of the stagnation point with space and time and the resulting flow reversals around the stagnation point cause no computational difficulties and the numerical tests show that the accuracy is better than required for practical problems.

### GENERAL OBJECTIVE

TO DEVELOP A GENERAL METHOD FOR COMPUTING UNSTEADY HEAT TRANSFER ON TURBINES BLADES  
SUBJECT TO NONUNIFORM ONSET VELOCITY



### APPROACH

INTERACTIVE BOUNDARY-LAYER THEORY BASED ON THE SOLUTION OF INVISCID AND VISCOUS FLOW  
EQUATIONS BY A NOVEL COUPLING PROCEDURE

Figure 1. - Approach to rotor wake heat-transfer problem.

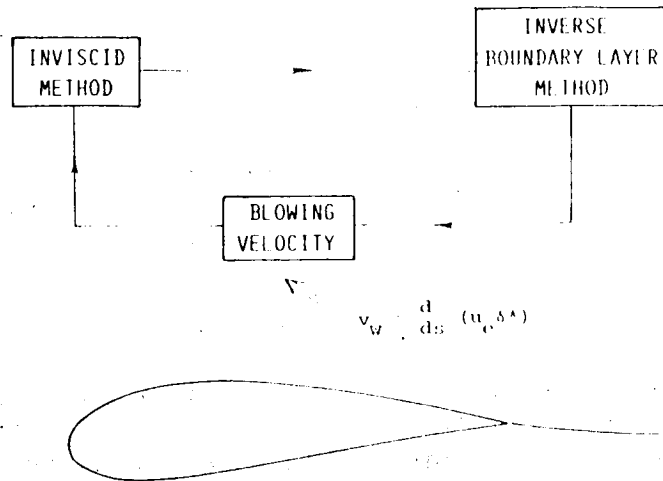


Figure 2. - Interactive scheme. Viscous calculations on the airfoil and in the wake are performed by a series of successive sweeps to establish new boundary conditions for the inviscid method.

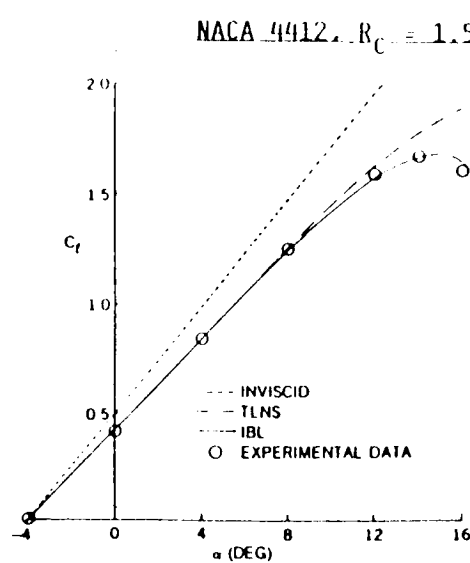


Figure 3. - Typical results for single airfoils.

GENERAL FORM OF EXTERNAL VELOCITY FIELD:

$$\frac{u_e}{u_\infty}(x, t) = A(\xi, \tau) [\xi - B(\tau)] \quad (1)$$

BOUNDARY-LAYER EQUATIONS FOR UNSTEADY FLOWS:

$$\frac{\partial u}{\partial x} + \frac{\partial v}{\partial y} = 0 \quad (2)$$

$$\frac{\partial u}{\partial \tau} + u \frac{\partial u}{\partial x} + v \frac{\partial u}{\partial y} = \frac{\partial u_e}{\partial \tau} + u_e \frac{\partial u_e}{\partial x} + v \frac{\partial}{\partial y} \left( b \frac{\partial u}{\partial y} \right) \quad (3)$$

$$\frac{\partial T}{\partial \tau} + u \frac{\partial T}{\partial x} + v \frac{\partial T}{\partial y} = \frac{v}{Pr} \frac{\partial}{\partial y} \left( c \frac{\partial T}{\partial y} \right) \quad (4)$$

$$y = 0, \quad u = v = 0, \quad T = T_w(x); \quad (5a)$$

$$y = \delta, \quad u = u_e(x, t), \quad T = T_e \quad (5b)$$

$$b = 1 + \frac{c_m}{v}, \quad c = 1 + \frac{c_m}{v} \frac{Pr}{Pr_t} \quad (6)$$

$$(bf'')' + f''\theta + \frac{\partial w}{\partial \tau} + w \frac{\partial w}{\partial \xi} = \frac{\partial f'}{\partial \tau} + f' \frac{\partial f'}{\partial \xi} \quad (7)$$

$$\frac{1}{Pr} (cG')' + G'\theta + m(1 - G)f' = \frac{\partial G}{\partial \tau} + f' \frac{\partial G}{\partial \xi} \quad (8)$$

$$\eta = 0, \quad f = f' = G = 0; \quad \eta = \eta_e, \quad f' = w, \quad G = 1 \quad (9)$$

"CHARACTERISTIC" FORM OF THE EQUATIONS:

WRITE THE EQUATIONS ALONG THE LOCAL STREAMLINES

$$d\tau = d\xi/f'$$

$$(bf'')' + f''\theta + \frac{\partial w}{\partial \tau} + w \frac{\partial w}{\partial \xi} = \lambda \frac{\partial f'}{\partial s} \quad (10)$$

$$\frac{1}{Pr} (cG')' + G'\theta + m(1 - G)f' = \lambda \frac{\partial G}{\partial s} \quad (11)$$

$$\eta = 0, \quad \theta = f' = G = 0, \quad \eta = \eta_e, \quad f' = w, \quad G = 1 \quad (12)$$

$$\lambda = \sqrt{1 + (f')^2}, \quad \beta = \tan^{-1} f' \quad (13)$$

Figure 4. - Description of the method.

- PRESENT CONTRIBUTION ADDRESSES THE NUMERICAL SOLUTION OF THE BOUNDARY-LAYER EQUATIONS FOR A GIVEN PRESSURE DISTRIBUTION AND ITS EVALUATION FOR MODEL LAMINAR AND TURBULENT FLOWS.
- FOR NONUNIFORM ONSET VELOCITIES, THE STAGNATION POINT LOCATION  $\xi_s$  VARIES WITH SPACE AND TIME, I.E. FOR AN OSCILLATING AIRFOIL WHOSE  $u_\infty$  NEAR THE LEADING EDGE IS

$$u_e \sim \frac{z + z_0}{\sqrt{1 + z^2}} (1 + c \sin \omega \tau)$$

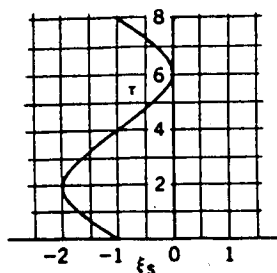
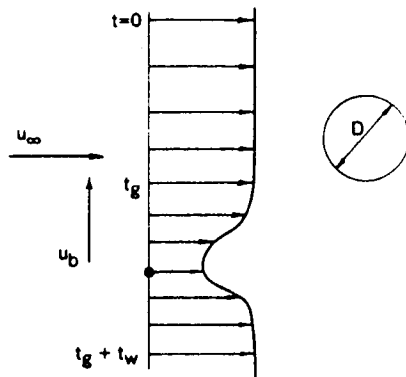


Figure 5. - Variation of stagnation point with time.



$$A(\tau) = \frac{[h^2 + 10(St)^2(1-h)^2]^{1/2}}{h} \quad (14)$$

$$B(\tau) = \tan^{-1} [3.3St (\frac{1}{h} - 1)] \quad (15)$$

$$h = \frac{1 + u_m}{2} + \frac{1 - u_m}{2} \cos[\pi(1 - 100 St \tau)] \quad (16)$$

Figure 6. - Rotor wake model.

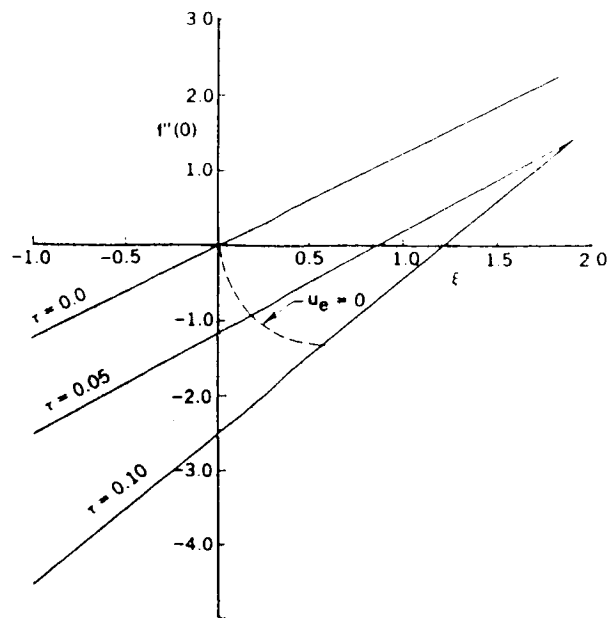


Figure 7. - Shear stress results for rotor wake model.

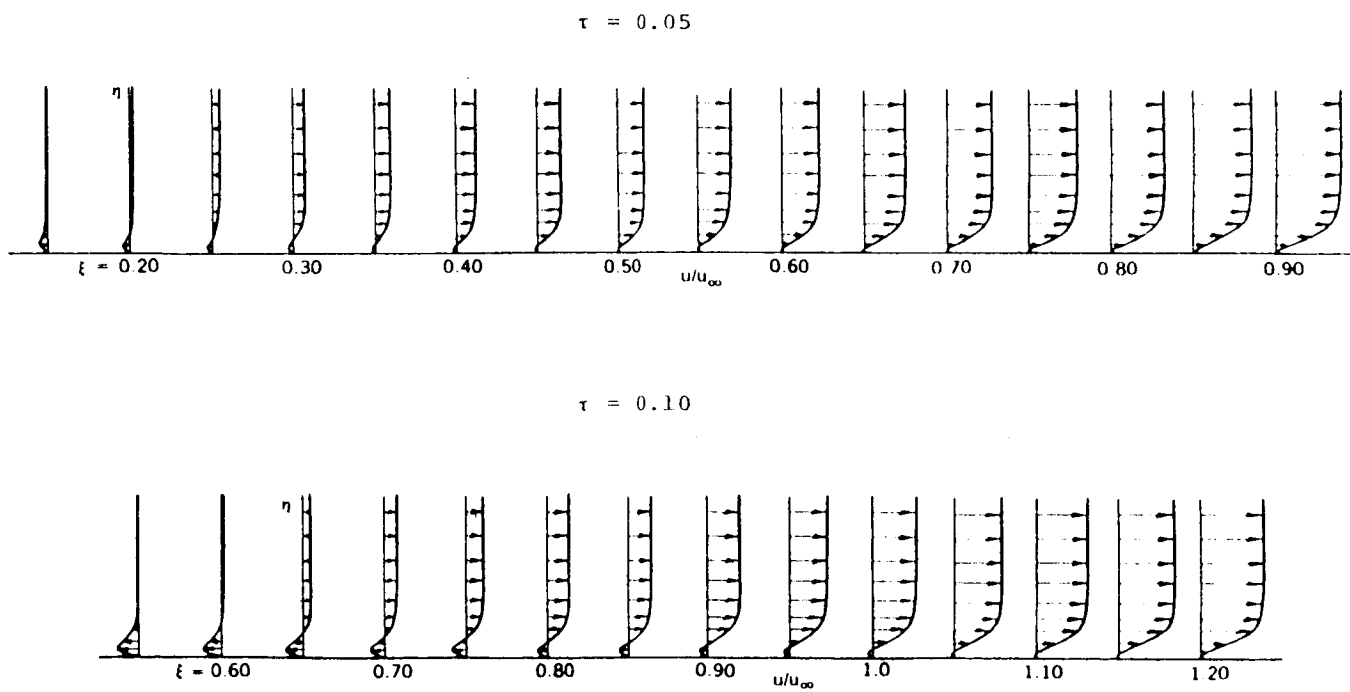


Figure 8. - Flow reversal results for rotor wake model.